Mon. Not. R. Astron. Soc. **381,** L65–L69 (2007) doi:10.1111/j.1745-3933.2007.00368.x

GRB 060206 and the quandary of achromatic breaks in afterglow light curves

P. A. Curran,[1⋆] A. J. van der Horst,[1] R. A. M. J. Wijers,[1] R. L. C. Starling,[2] A. J. Castro-Tirado,[3] J. P. U. Fynbo,[4] J. Gorosabel,[3] A. S. Järvinen,[5,6] D. Malesani,[4,7] E. Rol,[2] N. R. Tanvir,[2] K. Wiersema,[1] M. R. Burleigh,[2] S. L. Casewell,[2] P. D. Dobbie,[8] S. Guziy,[9] P. Jakobsson,[10] M. Jelínek,[3] P. Laursen,[4] A. J. Levan,[11] C. G. Mundell,[12] J. Näränen[13] and S. Piranomonte[14]

[1]*Astronomical Institute, University of Amsterdam, Kruislaan 403, 1098 SJ Amsterdam, the Netherlands*
[2]*Department of Physics and Astronomy, University of Leicester, University Road, Leicester LE1 7RH*
[3]*Instituto de Astrofísica de Andalucía (IAA-CSIC), PO Box 3004, 18080 Granada, Spain*
[4]*Dark Cosmology Centre, Niels Bohr Institute, University of Copenhagen, Juliane Maries Vej 30, 2100 Copenhagen, Denmark*
[5]*Astrophysikalisches Institut Potsdam, An der Sternwarte 16, D-14482 Potsdam, Germany*
[6]*Astronomy Division, PO Box 3000, FI-90014 University of Oulu, Finland*
[7]*International School for Advanced Studies (SISSA/ISAS), via Beirut 2-4, I-34014 Trieste, Italy*
[8]*Anglo-Australian Observatory, PO Box 296, Epping, NSW 1710, Australia*
[9]*Kalinenkov Astronomical Observatory, Nikolaev State University, Nikolskaya 24, 54030, Ukraine*
[10]*Centre for Astrophysics Research, University of Hertfordshire, College Lane, Hatfield, Herts AL10 9AB*
[11]*Department of Physics, University of Warwick, Coventry CV4 7AL*
[12]*Astrophysics Research Institute, Liverpool John Moores University, Twelve Quays House, Birkenhead CH41 1LD*
[13]*Nordic Optical Telescope, Apartado 474, Santa Cruz de La Palma, Spain*
[14]*INAF, Osservatorio Astronomico di Roma, via Frascati 33, I-00040, Monteporzio Catone (Roma), Italy*

Accepted 2007 July 17. Received 2007 June 26; in original form 2007 June 8

ABSTRACT

Gamma-ray burst afterglow observations in the *Swift* era have a perceived lack of achromatic jet breaks compared with the *BeppoSAX* era. We present our multi-wavelength analysis of GRB 060206 as an illustrative example of how inferences of jet breaks from optical and X-ray data might differ. The results of temporal and spectral analyses are compared, and attempts are made to fit the data within the context of the standard blast wave model. We find that while the break appears more pronounced in the optical and evidence for it from the X-ray alone is weak, the data are actually consistent with an achromatic break at about 16 h. This break and the light curves fit standard blast wave models, either as a jet break or as an injection break. As the pre-*Swift* sample of afterglows are dominated by optical observations, and in the *Swift* era most well-sampled light curves are in the X-ray, caution is needed when making a direct comparison between the two samples, and when making definite statements on the absence of achromatic breaks.

Key words: radiation mechanisms: non-thermal – gamma-rays: bursts – X-rays: individual: GRB 060206.

1 INTRODUCTION

Gamma-ray bursts (GRBs) are well described by the blast wave, or fireball, model (Rees & Mészáros 1992; Mészáros, Rees & Wijers 1998), which details their temporal and spectral behaviour. In this model GRB afterglow emission is created by shocks when a collimated ultrarelativistic jet ploughs into the circumburst medium, driving a blast wave ahead of it. This causes a non-thermal spectrum widely accepted to be synchrotron emission, with characteristic power-law slopes and spectral break frequencies. The signature of the collimation is an achromatic temporal steepening or 'jet break' at ∼1 d in an otherwise decaying, power-law light curve. The level of collimation, or jet opening angle, has important implications for the energetics of the underlying physical process.

Since the launch of the *Swift* satellite (Gehrels et al. 2004), this standard picture has been called into question by the rich and novel phenomena discovered in both the early and late light curves

⋆E-mail: pcurran@science.uva.nl

(e.g. Nousek et al. 2006). Here we focus on the perceived lack of achromatic temporal breaks in the *Swift* era, up to weeks in some bursts (e.g. Panaitescu et al. 2006; Burrows & Racusin 2007), which calls into question the effects of collimation and therefore the energy requirements of progenitor models. Some bursts show no evidence for breaks in either optical or X-ray, while others show clear breaks in one regime without any apparent accompanying break in the other. Even in those bursts where an achromatic break is observed, they may not be consistent with a jet break as predicted by the blast wave model (e.g. GRB 060124, Curran et al. 2007). We should note that our expectations of the observable signature of a jet break, including the fact that it ought to be perfectly achromatic, are based on highly simplified models, notably those of Rhoads (1997, 1999) and Sari, Piran & Halpern (1999), and break observations, pre-*Swift*, that were based predominantly in one regime (i.e. optical). So apart from well-sampled multi-regime observations, more realistic models and simulations of the light curves, beyond the scope of this Letter, will also be required to settle this issue.

As the apparent lack of observed achromatic breaks is an important issue in the *Swift* era, we will discuss the perceived presence and absence of these achromatic breaks, using the long burst GRB 060206 as an illustrative example. We present our multi-wavelength analysis of the well-sampled afterglow from X-ray to optical wavelengths. In Section 2 we introduce our observations, while in Section 3 we present the results of our temporal and spectral analyses. In Section 4 we discuss these results in the overall context of the blast wave model of GRBs, and we summarize our findings in Section 5.

2 OBSERVATIONS

Throughout, we use the convention that a power-law flux is given as $F_\nu \propto t^{-\alpha}\nu^{-\beta}$, where α is the temporal decay index and β is the spectral index. All errors and uncertainties are quoted at the 1σ confidence level.

2.1 Optical

Optical observations in the *B*, *V*, *R* and *I* bands were obtained at the 2.5-m Nordic Optical Telescope (NOT), the 2.5-m Isaac Newton Telescope (INT) and 3.6-m Telescopio Nazionale Galileo (TNG) on La Palma, the 1.5-m Observatorio de Sierra Nevada (OSN) in Granada, Spain, the 1.8-m Astrophysical Observatory of Asiago, Italy, and the 2.0-m Faulkes Telescope North (FTN) at Haleakala, Hawaii (Table 1). The optical counterpart was identified in the initial *R*-band frames; however, no counterpart was detected in the *B*-band frames, in agreement with the significant level of line blanketing associated with the Lyman forest at a redshift of $z = 4.048$ (Fynbo et al. 2006): the fluxes of the *B*, *V* and *R* bands were reduced to 8, 50 and 88 per cent, respectively, of their true values (Madau 1995). The field was calibrated via a standard Landolt (1992) field taken by the OSN on a photometric night. Differential photometry was carried out relative to a number of stars within ∼5 arcmin of the burst, with resulting deviations less than the individual errors. The photometric calibration error is included in error estimates. We combined our *R*-band data with those already published from the RAPTOR and MDM telescopes (Woźniak et al. 2006; Stanek et al. 2007; where MDM was shifted +0.22 mag as in Monfardini et al. 2006) to extend the optical light curve past 1×10^6 s since trigger.

Table 1. Optical observations of GRB 060206. Magnitudes are given with 1σ errors or as 3σ limits.

$T_{\rm mid}$ (s)	$T_{\rm exp}$ (s)	Band	Magnitude
78 373	1200	OSN *B*	> 22.7
81 977	300	OSN *V*	20.96 ± 0.18
816	60	INT *R*	17.28 ± 0.13
981	180	INT *R*	17.31 ± 0.14
1074	300	NOT *R*	17.45 ± 0.09
1391	600	INT *R*	17.44 ± 0.12
1468	300	NOT *R*	17.43 ± 0.08
1853	180	INT *R*	17.49 ± 0.12
1862	300	NOT *R*	17.55 ± 0.09
5363	120	OSN *R*	16.62 ± 0.09
8300	300	INT *R*	17.03 ± 0.14
18 360	1200	FTN *R*	17.90 ± 0.04
29 940	1050	FTN *R*	18.50 ± 0.02
68 235	1200	Asiago *R*	19.64 ± 0.04
75 990	180	OSN *R*	19.87 ± 0.15
80 917	180	OSN *R*	19.87 ± 0.09
82 225	180	OSN *R*	19.91 ± 0.07
160 557	1200	Asiago *R*	20.92 ± 0.07
209 760	960	FTN *R*	21.23 ± 0.10
248 617	1500	OSN *R*	21.81 ± 0.28
382 560	960	FTN *R*	> 21.9
687 323	120	TNG *R*	23.19 ± 0.25
1 121 271	600	NOT *R*	24.66 ± 0.41
2 160 836	600	NOT *R*	> 23.6
5529	120	OSN *I*	15.77 ± 0.12
82 424	180	OSN *I*	19.18 ± 0.15

2.2 X-ray

The X-ray event data from the *Swift* X-Ray Telescope (XRT; Burrows et al. 2005) were initially processed with the FTOOL XRTPIPELINE (v0.9.9). Source and background spectra from 0.3 to 10.0 keV in windowed timing (WT) and photon counting (PC) mode were extracted for analysis with XSPEC, while the pre-reduced XRT light curve was downloaded from the on-line repository (Evans et al. 2007).

3 RESULTS

3.1 Light curves

Visual inspection of the optical light curve (Fig. 1) clearly shows significant re-brightening at ∼4000 s and a 'bump' at $\sim 1.7 \times 10^4$ s, after which there is a smooth decay with a break at $\sim 5 \times 10^4$ s (Woźniak et al. 2006; Monfardini et al. 2006; Stanek et al. 2007). Fitting a broken power law to the data after the 'bump' gives $\alpha_1 = 1.138 \pm 0.005$, $\alpha_2 = 1.70 \pm 0.06$, and places the break at $t_{\rm break} = 5.9 \pm 0.5 \times 10^4$ s ($\chi^2_\nu = 0.77$, 71 degrees of freedom, d.o.f.). It is plausible that the late data suffer from contamination due to the host galaxy which is estimated as $R \sim 24.6$ (Thöne et al., in preparation), and therefore we have included this in our model.

The X-ray light curve also displays a re-brightening at ∼ 4000 s (e.g. Monfardini et al. 2006) and a flattening after $\sim 10^6$ s which has been attributed to a nearby contaminating X-ray source (Stanek et al. 2007). We used the count rate light curve since, as we will show in Section 3.2, the X-ray data are best described by a single, unchanging spectral index, so converting to flux only adds uncertainties. The X-ray data from 4000 to 10^6 s were well fitted by a single

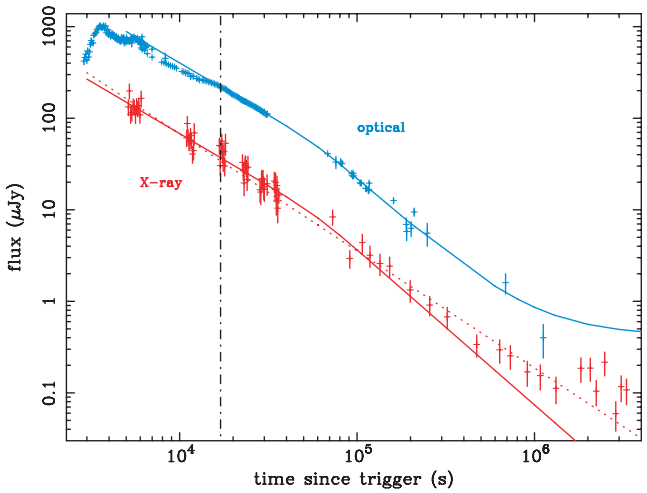

Figure 1. Optical (*R* band, upper blue crosses) and X-ray count rate (× 200, lower red crosses) light curves of GRB 060206. The solid lines show the smoothly broken power-law (with host correction) fit to the optical data to the right of the vertical dot–dashed line, and those same parameters scaled to the X-ray data. The dotted line shows a single power-law fit to the X-ray data.

Table 2. The temporal decay indices in X-ray and optical for a single power law, α, and a smoothly broken power law, α_1 and α_2, with a break time $t_{\rm break}$. Also listed are the spectral indices for X-ray, optical and combined X-ray/optical fits (Section 3).

	X-ray	Optical	Combined
α	1.28 ± 0.02	–	–
α_1	1.04 ± 0.10	1.138 ± 0.005	–
α_2	1.40 ± 0.07	1.70 ± 0.06	–
$t_{\rm break} \times 10^4$ s	$2.2^{+2.0}_{-0.8}$	4.9 ± 0.5	–
$\beta_{\rm pre\text{-}break}$	1.26 ± 0.06	0.84 ± 0.05	0.93 ± 0.01
$\beta_{\rm post\text{-}break}$	0.92 ± 0.09	1.4 ± 0.6	1.00 ± 0.06

power-law decay with $\alpha = 1.28 \pm 0.02$ ($\chi^2_\nu = 1.0$, 65 d.o.f.). However, we also fitted a broken power law with $\alpha_1 = 1.04 \pm 0.10$, $\alpha_2 = 1.40 \pm 0.7$, and a break time of $t_{\rm break} = 2.2^{+2.0}_{-0.8} \times 10^4$ s ($\chi^2_\nu = 0.79$, 63 d.o.f.), giving a marginal improvement. To test whether the X-ray is indeed consistent with the optical, we fixed the temporal slopes and break time to those of the optical and fitted the X-ray data. We find that these parameters well describe the X-ray data ($\chi^2_\nu = 0.94$, 66 d.o.f.; Fig. 1). The results of our temporal fits are summarized in Table 2.

3.2 Spectral analysis

The XRT spectra were fitted with an absorbed power law and, in both the WT and PC mode data, a significant amount of absorption over the Galactic value was required. This excess extinction may be explained by host extinction in the rest frame of the burst. For the WT mode data (i.e. pre-break) a spectral index of $\beta_{\rm X} = 1.26 \pm 0.06$ was found ($\chi^2_\nu = 1.10$, 94 d.o.f.), while the PC mode data (i.e. post-break) were found to have a spectral index of $\beta_{\rm X} = 0.92 \pm 0.09$ ($\chi^2_\nu = 0.93$, 59 d.o.f.).

Two optical spectral indices were found by fitting the optical spectral energy distributions (SEDs) at $\sim 1.0 \times 10^4$ and $\sim 8.2 \times 10^4$ s (i.e. pre- and post-break). For the pre-break analysis we used the near-infrared data ($JHK_{\rm S}$) of Alatalo, Perley & Bloom (2006) and the shifted *R*-band data, at that time, of Stanek et al. (2007). For the post-break SED we used our *V*-, *R*- and *I*-band data. All data were converted to fluxes and corrected for a Galactic extinction of $E(B-V) = 0.013$ (Schlegel, Finkbeiner & Davis 1998) and line blanketing due to the Lyman forest. We find optical spectral indices of $\beta_{\rm opt} = 0.84 \pm 0.05$ and 1.4 ± 0.6 for pre- and post-break, respectively.

To constrain these values further, we used the simultaneous X-ray and optical fitting detailed in Starling et al. (2007a). In this method, the optical to X-ray SED is fitted in count space, incorporating the measured metallicity (Fynbo et al. 2006) and including the effect of host galaxy extinction. The above optical data points were augmented by X-ray data at the given times: the pre-break SED by one orbit of XRT data and the post-break SED by $\sim 3 \times 10^4$ s of data. From this we find that both epochs are well described by a single spectral power law with $\beta = 0.93 \pm 0.01$ and 1.00 ± 0.06, respectively, in agreement with each other and with our previous values of $\beta_{\rm opt}$ and $\beta_{\rm X}$, but inconsistent with the interpretation of a possible spectral change in the optical between the two epochs. These results are shown in Table 2 and agree, within the errors, with those of Monfardini et al. (2006).

4 DISCUSSION

We have shown that the well-sampled X-ray afterglow can be described by a single power-law decay, although a broken power law, which gives temporal indices and a break time similar to those in the optical, is as good a fit. While it is difficult to accommodate the single power-law decay in the framework of the blast wave model, an achromatic broken power-law decay can be interpreted in terms of a jet break or an energy injection break, which we will now discuss in the context of the blast wave model [for a review and mathematical relations see e.g. Zhang & Mészáros (2004)].

The spectral indices of the optical to X-ray spectrum are constant before and after the optical break, i.e. at ∼2.9 and ∼ 23 h with the break at ∼16 h (∼3 h in the rest frame) after the burst. This indicates that the temporal break is not caused by the passage of a break frequency through the optical regime in the broad-band spectrum. The conclusion one can draw from this is that the break is caused by a change in the dynamics of the jet, e.g. the cessation of the energy injection phase or the beginning of the jet-spreading phase (the jet break interpretation). Assuming that the optical emission and X-ray emission are caused by the same mechanism, the X-ray light curve is expected to show a break at the same time as the optical.

We note that Monfardini et al. (2006) ascribe the dynamical change of the blast wave to a change in the circumburst density profile, the blast wave breaking out of a homogeneous medium into a stellar wind-like environment. This model agrees with the observed spectral and temporal slopes, but is not expected from the immediate environment models of GRB progenitors, which predict a transition from a wind-like to a homogeneous medium, and not the converse (e.g. Wijers 2001; Ramirez-Ruiz et al. 2005). In the following we explore the two possible explanations that we propose for the SEDs and light curves of the afterglow of this burst, a jet break and an energy injection break.

4.1 Jet break versus energy injection

From the SED spectral indices the power-law index of the electron energy distribution, p, can be determined. For both possible explanations the interpretation of the SEDs is the same, in that the single power-law SED from the optical to X-rays is either in between the

peak frequency, ν_m, and the cooling frequency, ν_c, or above both frequencies. In the first case $p = 3.00 \pm 0.12$, while in the latter case $p = 2.00 \pm 0.12$, using the spectral slopes from the optical to X-ray fit in count-space at 23 h after the burst.

In the jet break interpretation of the achromatic break, the blast wave is moving ultrarelativistically, but decelerating, before the break. When the Lorentz factor of the blast wave drops below the inverse half-opening angle of the jet, the observer starts to see the whole jet and the jet begins to spread sideways, giving rise to the so-called jet break. If both the X-ray and optical regimes are situated between ν_m and ν_c, the temporal slope before the break, given the value of p derived from the SED, is $\alpha = 3(p-1)/4 = 1.50 \pm 0.09$ or $\alpha = (3p-1)/4 = 2.00 \pm 0.09$, for a homogeneous or a stellar wind environment, respectively. The post-break slope would then be $\alpha = p = 3.00 \pm 0.12$. All these slopes are too steep compared with the observed temporal slopes. If, however, both observing regimes are above ν_m and ν_c, the pre-break slope is $\alpha = (3p-2)/4 = 1.00 \pm 0.09$, while the post-break slope is $\alpha = p = 2.00 \pm 0.12$. The pre-break slope in this case is consistent with the observed slopes. The observed post-break slopes are slightly shallower than expected, but they are consistent within 3σ, although further steepening to an asymptotic value of $\alpha = p$ cannot be ruled out. To conclude, in the jet break interpretation we find that $p = 2.00 \pm 0.12$ and $\nu_{m,c} < \nu_{opt,X}$, but we cannot say anything about the structure of the circumburst medium, i.e. homogeneous or wind, since that requires that the observing frequencies are below ν_c.

If the achromatic break is interpreted as the cessation of an extended energy injection phase, the post-break slopes are given by the expressions for an ultrarelativistic blast wave. In this case, if both observing frequencies are situated in between ν_m and ν_c, the temporal slopes after the break are $\alpha = 3(p-1)/4 = 1.50 \pm 0.09$ (homogeneous medium) or $\alpha = (3p-1)/4 = 2.00 \pm 0.09$ (stellar wind). If both observing frequencies are situated above the spectral break frequencies, the temporal slope is $\alpha = (3p-2)/4 = 1.00 \pm 0.09$, regardless of the circumburst medium structure. Comparing these numbers with the observed post-break slopes, the observations are best fitted when $\nu_m < \nu_{opt,X} < \nu_c$ and hence $p = 3.00 \pm 0.12$, and the ambient medium is homogeneous. Assuming that the energy injection can be described as $E \propto t^q$, the flattening of the light curves before the break is given by $\Delta\alpha = (p+3)/4 \times q \simeq 1.5 \times q$, which gives $q \sim 0.3$ from the observed average flattening of $\Delta\alpha \sim 0.4$.

4.2 Energetics

In general, the jet break time is related to the half-opening angle of the jet, from which the isotropic equivalent energy can be converted into the collimation corrected energy. If we interpret the achromatic break at $\sim$16 h as a jet break, the half-opening angle of the jet is found to be $\theta_0 = 0.075 \times (E_{52}/n_0)^{-1/8} \sim 4^\circ$ or $\theta_0 = 0.11 \times (E_{52}/A_*)^{-1/4} \sim 7^\circ$, for a homogeneous medium or a stellar wind environment, respectively (Panaitescu & Kumar 2002). If we adopt the energy injection interpretation, the observations indicate that there has not been a jet break up to 10 d after the burst, which results in a lower limit on the jet half-opening angle of $\theta_0 > 0.22 \times (E_{52}/n_0)^{-1/8} \sim 13^\circ$. In all these expressions for the opening angle, E_{52} is the isotropic equivalent blast wave energy in units of 10^{52} erg; n_0 is the homogeneous circumburst medium density in cm^{-3}; and $A_* = \dot{M}/(4\pi v_w^2)$, with $\dot{M}$ the mass-loss rate in 10^{-5} M$_\odot$ per year and v_w the stellar wind velocity in 10^3 km s^{-1}. These typical values for the energy and density (Panaitescu & Kumar 2002) are in agreement with the constraints on the values for ν_m and ν_c compared to the observing frequencies. Also the fractional energies of radiating electrons and magnetic field, ε_e and ε_B respectively, have typical values of $\sim$0.1, although in the energy injection interpretation $\varepsilon_B \sim 10^{-3.5}$, which has been found for other bursts. With these opening angles we can convert the isotropic equivalent gamma-ray energy of 6×10^{52} erg (Palmer et al. 2006) into collimation corrected energies of $2\text{–}4 \times 10^{50}$ erg for the jet break interpretation and $>10^{51}$ erg for the energy injection interpretation, consistent with the energy distribution of other bursts (Frail et al. 2001).

4.3 Implications

Many previously studied jet breaks do not display sharp changes in the temporal decay index, but show a shallow roll-over from asymptotic values which is described by a smoothly broken power law. The prototypical example of such a break is GRB 990510 for which well-sampled *B*-, *V*-, *R*- and *I*-band light curves display an achromatic break (e.g. Stanek et al. 1999). This is accepted as a jet break even though the X-ray light curve as measured by *BeppoSAX* (Kuulkers et al. 2000) is satisfactorily described by a single power law. A break at X-ray frequencies at the same time as the optical break is, however, not ruled out, and the temporal slopes before and after that break are similar in the optical and X-rays. In the analysis of GRB 060206 we are seeing the same phenomenon: the optical light curve displays a break, while the X-ray is satisfactorily described by a single power-law fit, although a broken power law is not ruled out. However, an X-ray break is necessary to explain the afterglow when interpreting it in the context of the standard blast wave model. A similar issue has been addressed in SED fits by Starling et al. (2007b), where adding a cooling break to some SEDs gives only a marginal improvement according to the statistical *F*-test, but is necessitated by considerations of the physical model. This has significant implications for the analysis of the myriad of X-ray light curves that the *Swift* satellite has afforded us. For those X-ray light curves extending up to $\sim$1 d or longer, for which we do not have well-sampled optical light curves, caution is required when making claims about the absence of breaks in isolation, without considering physical interpretations. This is particularly important when performing statistical analyses on a large sample of temporal and spectral slopes, for making collimation corrected energy estimates, and for using GRBs as standard candles.

5 CONCLUSION

We identify a possible achromatic break in the X-ray and optical light curves of GRB 060206 at $\sim$16 h, which is most successfully explained by a change in the dynamics of the jet: either as a jet break or as a break due to the cessation of energy injection. Neither is favoured, as both are consistent with the blast wave model and the distribution of collimation corrected energies. The presence of a weak constant source near the afterglow in both X-rays and optical precludes, in this case, an examination of the light curves later than $\sim 10^6$ s. GRB 060206 was, up to now, assumed to have a chromatic break (i.e. a break only in the optical) since the X-ray data alone do not require a break. However, examining all X-ray and optical data until late times, we find that the optical and X-ray light curves are consistent with having the same break time and pre- and post-break temporal slopes. There is also no evidence of chromaticity from a comparison of pre- and post-break SEDs that encompass optical and X-ray data.

We should therefore be cautious in ruling out breaks as being achromatic from comparing the nominal fitted slopes. This issue is important for determining true GRB energies, but also has a strong

bearing on recent attempts to use GRBs for determining the geometry of the distant Universe. That said, there does seem to be a tendency, if not yet strongly significant, for the X-ray light curves to have less pronounced breaks. Both GRB 060206 and 990510, the achromatic break 'poster child', are examples of this. It would therefore be worthwhile to extend the sample of *Swift* bursts that have well-sampled late-time optical light curves, which would be helped by finding more afterglows in the anti-Sun direction. Also, more detailed theoretical models of jet breaks (likely involving numerical simulations of the jet dynamics) should be preformed to clarify whether jet breaks could vary somewhat between wavebands.

ACKNOWLEDGMENTS

We thank the referee for constructive comments. PAC, RAMJW and KW gratefully acknowledge the support of NWO under grant 639.043.302. MRB, ER and RLCS gratefully acknowledge support from PPARC. DM acknowledges the Instrument Centre for Danish Astrophysics. ASJ acknowledges the Wihuri foundation, Finland. This work was partially supported by the Spanish research programmes ESP2002-04124-C03-01 and AYA2004-01515. NOT is operated by Denmark, Finland, Iceland, Norway and Sweden, in the Observatorio del Roque de los Muchachos of the Instituto de Astrofísica de Canarias, Spain. The Dark Cosmology Centre is funded by the Danish National Research Foundation. We acknowledge benefits from collaboration within the EU FP5 Research Training Network 'Gamma-Ray Bursts: An Enigma and a Tool' (HPRN-CT-2002-00294). This work made use of data supplied by the UK *Swift* Science Data Centre at the University of Leicester and the High Energy Astrophysics Science Archive Research Center Online Service, provided by the NASA/GSFC.

REFERENCES

Alatalo K., Perley D., Bloom J. S., 2006, GRB Coord. Network, 4702
Burrows D. N., Racusin J., 2007, Il Nuovo Cim. C, in press (arXiv:astro-ph/0702633)
Burrows D. N. et al., 2005, Space Sci. Rev., 120, 165
Curran P. A., Kann D. A., Ferrero P., Rol E., Wijers R. A. M. J., 2007, Il Nuovo Cim. C, in press (arXiv:astro-ph/0610067)
Evans P. A. et al., 2007, A&A, 469, 379
Frail D. A. et al., 2001, ApJ, 562, L55
Fynbo J. P. U. et al., 2006, A&A, 451, L47
Gehrels N. et al., 2004, ApJ, 611, 1005
Kuulkers E. et al., 2000, ApJ, 538, 638
Landolt A. U., 1992, AJ, 104, 340
Madau P., 1995, ApJ, 441, 18
Mészáros P., Rees M. J., Wijers R. A. M. J., 1998, ApJ, 499, 301
Monfardini A. et al., 2006, ApJ, 648, 1125
Nousek J. A. et al., 2006, ApJ, 642, 389
Palmer D. et al., 2006, GRB Coord. Network, 4697
Panaitescu A., Kumar P., 2002, ApJ, 571, 779
Panaitescu A., Mészáros P., Burrows D., Nousek J., Gehrels N., O'Brien P., Willingale R., 2006, MNRAS, 369, 2059
Ramirez-Ruiz E., García-Segura G., Salmonson J. D., Pérez-Rendón B., 2005, ApJ, 631, 435
Rees M. J., Mészáros P., 1992, MNRAS, 258, 41P
Rhoads J. E., 1997, ApJ, 487, L1
Rhoads J. E., 1999, ApJ, 525, 737
Sari R., Piran T., Halpern J. P., 1999, ApJ, 519, L17
Schlegel D. J., Finkbeiner D. P., Davis M., 1998, ApJ, 500, 525
Stanek K. Z., Garnavich P. M., Kaluzny J., Pych W., Thompson I., 1999, ApJ, 522, L39
Stanek K. Z. et al., 2007, ApJ, 654, L21
Starling R. L. C., Wijers R. A. M. J., Wiersema K., Rol E., Curran P. A., Kouveliotou C., Van der Horst A. J., Heemskerk M. H. M., 2007a, ApJ, 661, 787
Starling R. L. C., Van der HorstA. J., Rol E., Wijers R. A. M. J., Kouveliotou C., Wiersema K., Curran P. A., Weltevrede P., 2007b, A&A, in press (arXiv:0704.3718)
Wijers R. A. M. J., 2001, in Costa E., Frontera F., Hjorth J., eds, Gamma-ray Bursts in the Afterglow Era. Springer-Verlag, Berlin, p. 306
Woźniak P. R., Vestrand W. T., Wren J. A., White R. R., Evans S. M., Casperson D., 2006, ApJ, 642, L99
Zhang B., Mészáros P., 2004, Int. J. Mod. Phy. A, 19, 2385

This paper has been typeset from a TEX/LATEX file prepared by the author.